S & M 0764

Preparation of Mesoporous and Meso-macroporous SnO_2 Powders and Application to H_2 Gas Sensors

Luyang Yuan, Takeo Hyodo, Yasuhiro Shimizu[1,*] and Makoto Egashira[1]

Graduate School of Science and Technology, Nagasaki University,
1-14 Bunkyo-machi, Nagasaki 852-8521, Japan
[1]Faculty of Engineering, Nagasaki University, 1-14 Bunkyo-machi, Nagasaki 852-8521, Japan

Mesoporous SnO_2 (mp-SnO_2) and meso-macroporous SnO_2 (m·mp-SnO_2) pellet-type gas sensors were fabricated by the sol-gel method employing $SnCl_4 \cdot 5H_2O$ as a Sn source. The mesoporous structure was controlled by $C_{20}H_{37}O_7SNa$, while the macroporous structure was controlled by polymethylmethacrylate (PMMA) microspheres. The introduction of macropores by the addition of PMMA microspheres into mp-SnO_2 tends to increase the pore diameter and crystallite size. The large amount of macropores introduced into mp-SnO_2 sensors by the addition of PMMA microspheres in the preparation process significantly increased the resistance of all the sensors. Among all those tested, the mp-SnO_2 sensor with only 5 wt% Sb_2O_5 added exhibited the largest response at 400°C. The 70% response and recovery times could be reduced by the introduction of macropores.

1. Introduction

SnO_2 is well known to be the most important material for semiconductor gas sensors since it can be used to detect a wide variety of gases with high sensitivity, good stability and at low cost.[1–5] In recent years, particular focus has been directed to mesoporous (mp-) SnO_2 powders as sensor materials.[6–9] However, the poor thermal stability of the mesoporous structures of the mp-SnO_2 powders synthesized so far limits their applications to gas sensors, which are usually operated in the temperature range of 250 –500°C. In our previous study, thermally stable mp-SnO_2 powders were prepared by employing the self-assembly of a general surfactant as a template for the mesopore,[6,10] but the gas sensing properties of the mp-SnO_2 sensors were relatively lower than expected from their large specific surface area. In addition, we have demonstrated that well-developed macroporous ceramic films, which were prepared by a modified sol-

gel method employing polymethylmethacrylate (PMMA) microspheres as a template, showed excellent sensing properties to H_2.[11,12]

This study is, therefore, focused on preparing thermally stable mp-SnO_2 powders with submicron-sized macropores (m·mp-SnO_2 powders) by employing PMMA microspheres, with the aim of improving their H_2 sensing properties. In addition, the effects of the addition of SiO_2 and Sb_2O_5 to m·mp-SnO_2 on the H_2 gas sensing properties have also been examined.

2. Experimental

2.1 *Preparation of mp-SnO₂ and m·mp-SnO₂ powders*

mp-SnO_2 and m·mp-SnO_2 powders were prepared employing $SnCl_4 \cdot 5H_2O$ as a Sn source, and the mesoporous and macroporous structures were controlled by self-assemblies of sodium bis(2-ethylhexyl)sulfosuccinate (aerosol-OT, AOT, Kishida Chemical Co., Ltd.) and PMMA microspheres with a diameter of 800 nm (MP-1600, Soken Chem. & Eng. Co., Ltd.), respectively. The typical preparation procedures of mp-SnO_2 and m·mp-SnO_2 were as follows. A given amount of each constituent listed in Table 1 was mixed in 400 ml of ultrapure water and the pH value of the resulting mixture was adjusted, by adding an NH_3 aqueous solution, to be 8.5 in some cases. As for tetraethoxysilane (TEOS) and $SbCl_3$, the amounts required to produce the given amounts of SiO_2 and Sb_2O_5 were added to the solution. The mixed solutions were maintained at 20°C for 3 days. Thereafter, the solutions were evaporated in an oven at 80°C overnight. The resultant powders were then treated with a 0.1 mol dm^{-3} phosphoric acid solution for about 2 h, and then subjected to heat treatment at 650°C for 5 h in air. Hereafter, each sample will be referred to by its abbreviation listed in Table 1.

Table 1
Preparation conditions of mp-SnO_2 and m·mp-SnO_2.

Sample		Macropore template (PMMA)	Amount of MO added to SnO_2		pH adjusted
			MO: Sb_2O_5 (using $SbCl_3$)	MO: SiO_2 (using TEOS)	
mp-SnO_2	A	none	none	none	none
mp-SnO_2	A-S5	none	5 wt%	none	none
mp-SnO_2	A-TS5	none	5 wt%	9 wt%	8.5
m·mp-SnO_2	A-P	0.35 g	none	none	none
m·mp-SnO_2	A-PT	0.35 g	none	9 wt%	8.5
m·mp-SnO_2	A-PS5	0.35 g	5 wt%	none	none
m·mp-SnO_2	A-PTS1	0.35 g	1 wt%	9 wt%	8.5
m·mp-SnO_2	A-PTS5	0.35 g	5 wt%	9 wt%	8.5
m·mp-SnO_2	A-PTS10	0.35 g	10 wt%	9 wt%	8.5
m·mp-SnO_2	A-PTS17	0.35 g	17 wt%	9 wt%	8.5
m·mp-SnO_2	A-PTS33	0.35 g	33 wt%	9 wt%	8.5
m·mp-SnO_2	A-PTS50	0.35 g	50 wt%	9 wt%	8.5

The crystal phases of mp-SnO_2 and m·mp-SnO_2 powders were characterized by X-ray diffraction analysis (XRD; Rigaku, RINT2200), and the crystallite sizes were calculated using Scherrer's equation.

The specific surface area and pore size distribution were measured by the Brunauer-Emmett-Teller (BET) method using a N_2 sorption isotherm (Micromeritics, TriStar3000). The morphology of the powder pellets was observed by scanning electron microscopy (SEM; JEOL Ltd., JCM-5700).

2.2   *Fabrication of mp-SnO₂ and m·mp-SnO₂ sensors and measurement of their H₂ sensing properties*

mp-SnO_2 and m·mp-SnO_2 sensors were prepared as follows. Before heat treatment, the powder was molded into a pellet at a pressure of 1,000 kg cm^{-2}. Then, the pellet was calcined in air at 600°C for 5 h. A pair of Pt electrodes was fabricated on the pellet surface by screen printing. The gas sensing properties of the mp- and m·mp-SnO_2 pellet-type sensors to 1,000 ppm H_2 were measured at a flow rate of 0.1 dm^3 min^{-1} in the temperature range of 300–500°C. The magnitude of the response was defined as the ratio (R_a/R_g) of sensor resistance in air (R_a) to that in 1,000 ppm H_2 balanced with air (R_g).

3.   Results and Discussion

3.1   *Effects of introduction of macropores and/or various additives to mp-SnO₂ on the H₂ sensing properties*

3.1.1   *Characterization of mp-SnO₂ and m·mp-SnO₂ powders*

The pore size distribution and specific surface area (SSA) of mp-SnO_2 (samples A, A-S5 and A-TS5) and m·mp-SnO_2 (samples A-P, A-PT, A-PS5, A-PTS5) powders are shown in Fig. 1. Powder A, which was prepared without PMMA, TEOS or $SbCl_3$, showed a larger SSA of 152.1 m^2 g^{-1} and a larger pore volume of 0.145 cm^3 g^{-1} with a smaller centered pore diameter of ca. 2.9 nm than those of a conventional SnO_2 powder.[2–4] This means that powder A had a well-developed mesoporous structure. The addition of 5 wt% Sb_2O_5, i.e., A-S5, resulted in a slight increase in SSA (164.3 m^2 g^{-1}), while the addition of SiO_2 to the A-S5, i.e., A-TS5, markedly increased the SSA (200.2 m^2 g^{-1}) and reduced the centered diameter of the mesopores (to ca. 2 nm).

On the other hand, the introduction of macropores to powder A, i.e., A-P, slightly reduced the SSA (143.2 m^2 g^{-1}) and broadened the distribution of the mesopores with a larger centered pore diameter (ca. 4 nm), but the pore volume remained unchanged. These results support the finding that the introduction of macropores tends to increase the diameter of the mesopores, although the reason for this phenomenon is not clear at present. The addition of 5 wt% Sb_2O_5 to A-P, i.e., A-PS5, was hardly effective in modifying the mesoporous structure, while the addition of 9 wt% SiO_2 to A-P, i.e., A-PT, significantly increased the SSA and the pore volume with a smaller centered pore diameter (ca. 3.5 nm). The addition of 5 wt% Sb_2O_5 to A-PT, i.e., A-PTS5, resulted in a decrease in SSA without a marked change in the pore size distribution. Figure 2 shows SEM images of an mp-SnO_2 (A) pellet and representative m·mp-SnO_2 (A-PS5 and A-PTS5) pellets after calcination at 600°C for 5 h. For pellet A, a large amount
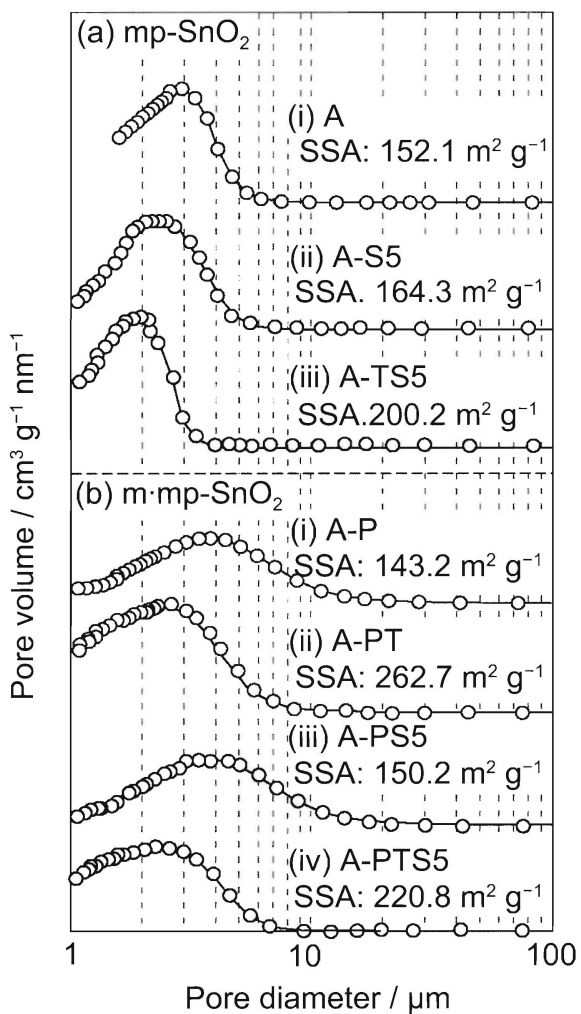
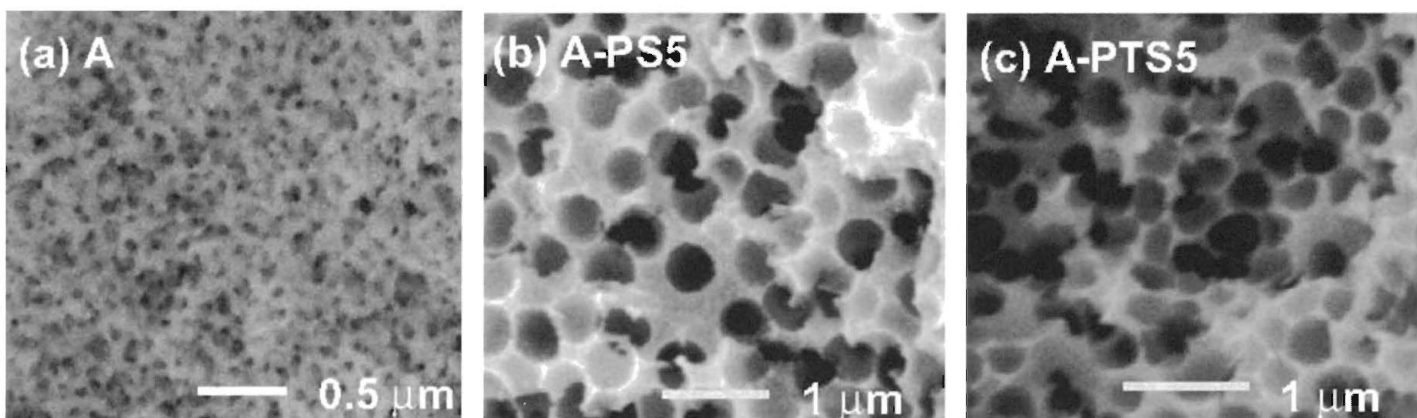Fig. 1.   Pore size distributions of mp- and m·mp-SnO$_2$ powders.

Fig. 2.   SEM images of mp- and m·mp-SnO$_2$ pellets.

of mesopores (23–69 nm in diameter) can be observed at the surface, but the similar size of mesopores was not confirmed in Fig. 1(a). This means that a large amount of small mesopores with a centered pore diameter of ca. 2.9 nm was well-developed inside the oxide walls. On the other hand, the formation of well-developed and spherical macropores in the range of 400–450 nm and 380–400 nm in diameter was observed at the surface of A-PS5 and A-PTS5, respectively. The morphology of such spherical macropores well reflected that of PMMA macrospheres (ca. 800 nm in diameter), but the ratio of their shrinkage was markedly high (ca. 47 and 59% for A-PS5 and A-PTS5, respectively).

Figure 3 shows XRD patterns of typical mp-SnO_2 and m·mp-SnO_2 powders after calcination at 650°C for 5 h. It is clear that all the powders have peaks corresponding to the SnO_2 crystalline phase (JCPDS 88-0287). The crystallite size (CS) increased with the introduction of macropores into mp-SnO_2 (from comparison of A and A-S5 with A-P and A-PS5, respectively). This is probably because the crystal growth was accelerated by the heat of the combustion of PMMA microspheres added as a macropore template. The crystal growth is also responsible for the increase in diameter of the mesopores observed for m·mp-SnO_2 in comparison with that of mp-SnO_2, as shown in Fig. 1. In addition, it was revealed that CS was markedly decreased by the addition of 5 wt% Sb_2O_5, from comparison of A and A-P with A-S5 and A-PS5, respectively, but no diffraction peaks other than SnO_2 were observed. This implies that the antimony added was sufficiently incorporated into the SnO_2 crystal lattice and a very small amount of Sb_2O_5 and/or antimony-based oxides prevented the crystal growth among SnO_2 crystallites.[16–18]
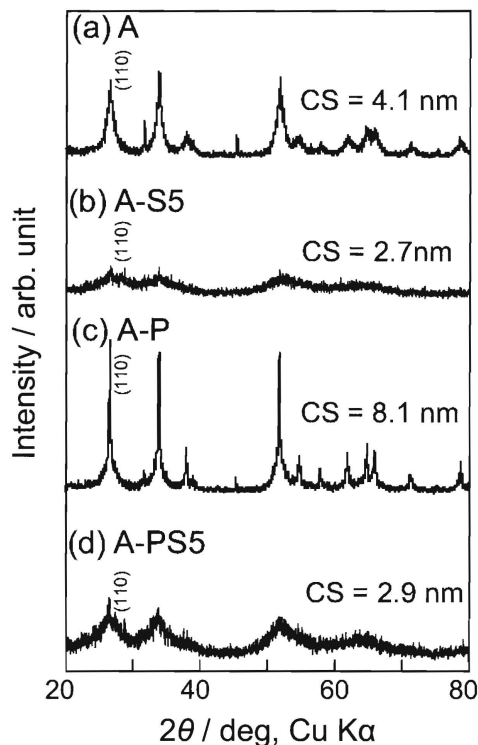

Fig. 3. XRD patterns of mp- and m·mp-SnO_2 powders.

3.1.2 *H₂ sensing properties of mp-SnO₂ and m·mp-SnO₂ sensors*

Figure 4 shows response transients of three types of m-SnO$_2$ sensor (A, A-S5, and A-TS5) and four types of m·mp-SnO$_2$ sensor (A-P, A-PS5, A-PT, and A-PTS5) to 1,000 ppm H$_2$ at 400°C. The introduction of a large amount of macropores into mp-SnO$_2$ sensors by the addition of PMMA microspheres in the preparation process markedly increased the resistance of all sensors (from comparison of A, A-S and A-TS5 with A-P, A-PS5 and A-PTS5, respectively), because these macropores greatly reduced the conductive pathways. In contrast, the addition of 5 wt% Sb$_2$O$_5$ reduced the sensor resistances, even though the crystallite size decreased upon Sb$_2$O$_5$ addition (see Fig. 3).
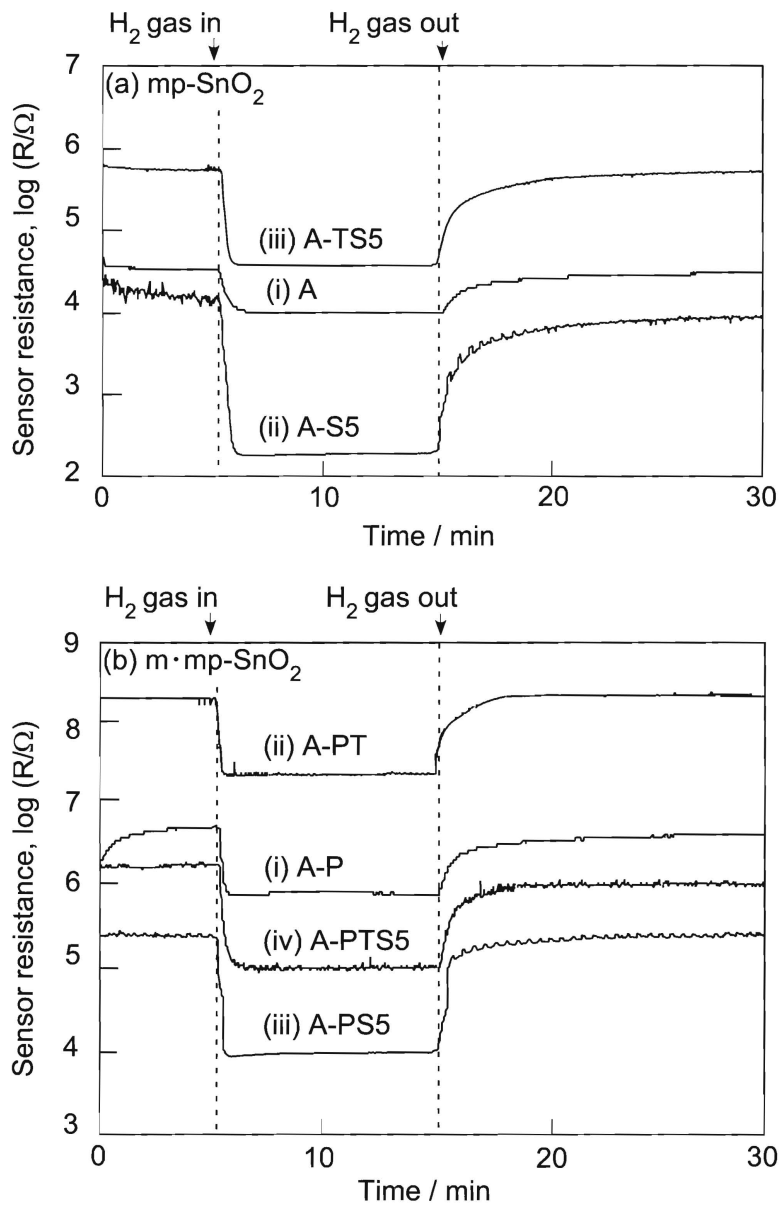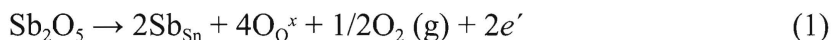

Fig. 4. Response transients of mp- and m·mp-SnO$_2$ sensors to 1,000 ppm H$_2$ at 400°C.

The resistance decrease can be explained by the valency control, i.e., partial substitution of Sn^{4+} sites with Sb^{5+} ions, producing free electrons, as described in eq. (1).[13–15]

$$Sb_2O_5 \rightarrow 2Sb_{Sn} + 4O_O{}^x + 1/2O_2 \text{ (g)} + 2e'$$ (1)

On the other hand, the simultaneous addition of 9 wt% SiO_2 with Sb_2O_5 increased the sensor resistances. The hydrolysis of TEOS, as a SiO_2 source, is generally slower than that of $SnCl_4$ and $SbCl_3$ as SnO_2 and Sb_2O_5 sources, respectively. Therefore, the SiO_2 probably segregated around the agglomerates of SnO_2 doped with Sb_2O_5, and then strictly limited the electron conduction among them.

To investigate the effects of the introduction of macropores and the addition of Sb_2O_5 and SiO_2 into mp-SnO_2 and m·mp-SnO_2 on the H_2 sensing properties, the operating temperature dependence of the magnitude of the H_2 response is also depicted in Fig. 5. Sensors A and A-P, which were prepared without TEOS or $SbCl_3$, showed relatively low H_2 responses, while the addition of 5 wt% Sb_2O_5 led to a large increase in H_2 response (see A-S5 and A-PS5 in Fig. 5). However, the simultaneous addition of 9 wt% SiO_2 with 5 wt%Sb_2O_5 decreased these H_2 responses (see A-PT, A-TS5 and A-PTS5). In contrast, the introduction of macropores does not seem to contribute to improving their responses sufficiently, from comparison of A, A-S5 and A-TS5 with A-P, A-PS5 and A-PTS5, respectively. Among these, it is apparent that some m·mp-SnO_2 sensors (A-P and A-PTS5) showed a slightly larger H_2 response than the mp-SnO_2 sensors (A and A-TS5), probably because the m·mp-SnO_2 powders had larger pore diameters than the mp-SnO_2 powders (see Fig. 1), and thus a larger number of active sites than the mp-SnO_2 powders.
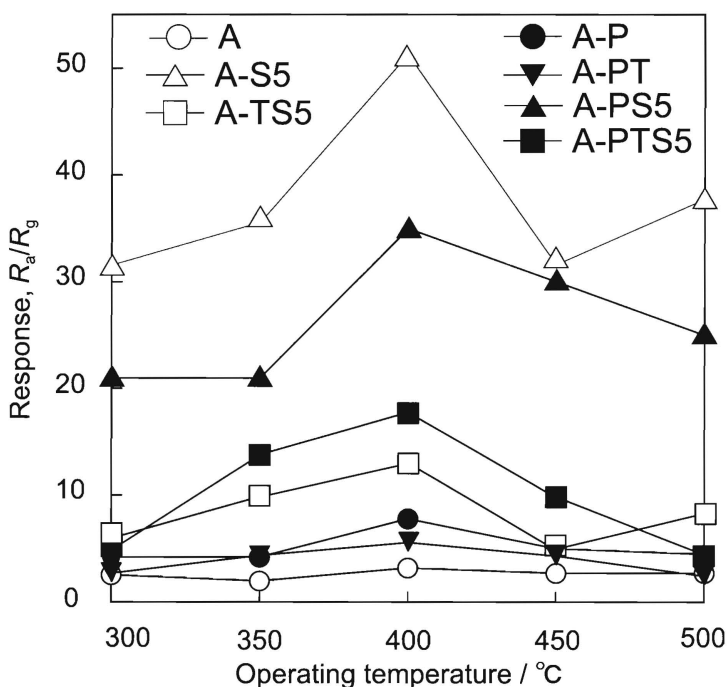

Fig. 5. Temperature dependences of response of representative mp- and m·mp-SnO_2 sensors to 1,000 ppm H_2.

On the other hand, A-S5 showed a relatively larger H_2 response than A-PS5, even though the pore diameter was smaller. This suggests that the existence of the additives (Sb_2O_5 or SiO_2) significantly affects the activity of gas reaction sites in m·mp-SnO_2.

The 70% response and recovery times of these sensors could be effectively reduced by the introduction of macropores, as summarized in Table 2. These results support the finding that the macropores markedly improved gas diffusivity in the m·mp-SnO_2 films and all gas molecules, such as H_2 as a reactant and H_2O as a product, easily access or more away from the active sites on the m·mp-SnO_2.

3.2   *Effects of Sb_2O_5 addition to m·mp-SnO_2 on their sensor properties*

The effects of the amount of Sb_2O_5 addition to m·mp-SnO_2 on the H_2 sensing properties were further investigated in detail, as shown in Fig. 6, since the addition of 5 wt% Sb_2O_5 markedly improved the H_2 responses of sensors A, A-P and A-PT. The addition of Sb_2O_5 up to 10 wt% was found to markedly reduce the sensor resistance in air. Therefore, it is recognized that the antimony was doped into the SnO_2. Beyond the addition of 10 wt%, the addition of Sb_2O_5 led to an increase in resistance with increasing

Table 2
Response and recovery times of representative mp-SnO_2 and m·mp-SnO_2 sensors.

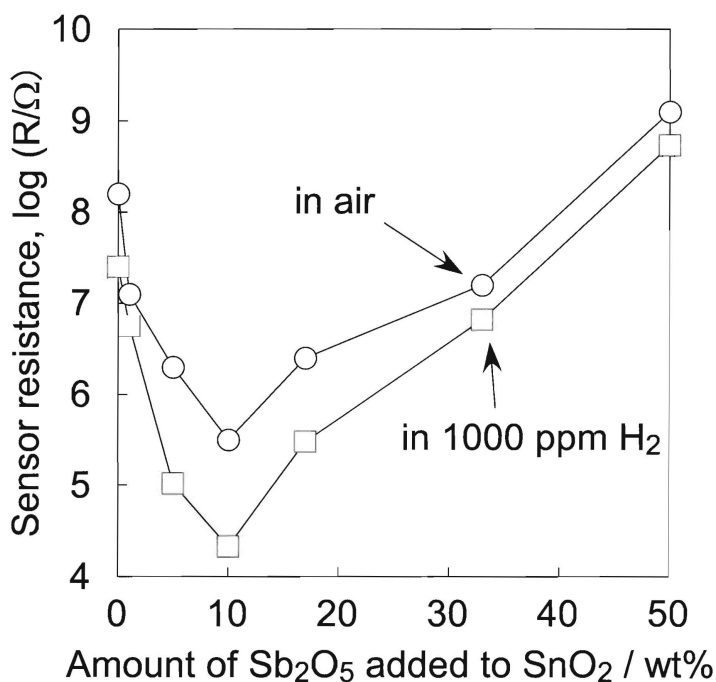| Sample No.	A	A-S5	A-S5	A-P	A-PT	A-PS5	A-PTS5
70% response time / s	23	24	19	13	17	20	17
70% recovery time / s	109	164	128	97	49	33	114

Fig. 6.   Variations in resistance of m·mp-SnO_2 sensors with amount of Sb_2O_5 added.

amount of Sb_2O_5 addition, probably owing to segregation of Sb_2O_5-based compounds due to the solubility limit of Sb_2O_5 into SnO_2, although these impurities were not confirmed by XRD due to low crystalline and/or small amounts thereof. Generally, it was reported that the solubility limit of Sb_2O_5 into SnO_2 was ca. 5 wt% and that 5 wt% doping results in the smallest CS[15–18] and the lowest resistance. The higher solubility limit of Sb_2O_5 observed in this study may result from localized heat from the combustion of the PMMA microspheres added in the preparation process, as discussed above.

Figure 7 shows the operating temperature dependence of the H_2 response of all Sb_2O_5-added m·mp-SnO_2 sensors (the amount of Sb_2O_5 addition: 0–50 wt%). A-PTS5 showed the highest H_2 response among them, irrespective of its low sensor resistance. This suggests a large acceleration of the combustion of H_2 with chemisorbed oxygen on the surface by the Sb_2O_5 doping. In addition, the response and recovery times of A-PTS5 were also the shortest among all the sensors (see Table 2). However, the sensor response of A-PTS5 was lower than those of A-S and A-PS5, as also shown in Fig. 5. This may arise from the fact that the existence of SiO_2 in m·mp-SnO_2 contributes to the increase in specific surface area, but also a reduction of the number of active sites on the SnO_2 surface. More detailed investigation on the surface chemistry of m·mp-SnO_2 added with Sb_2O_5 and SiO_2 will be carried to clarify the changes in their gas sensing properties.
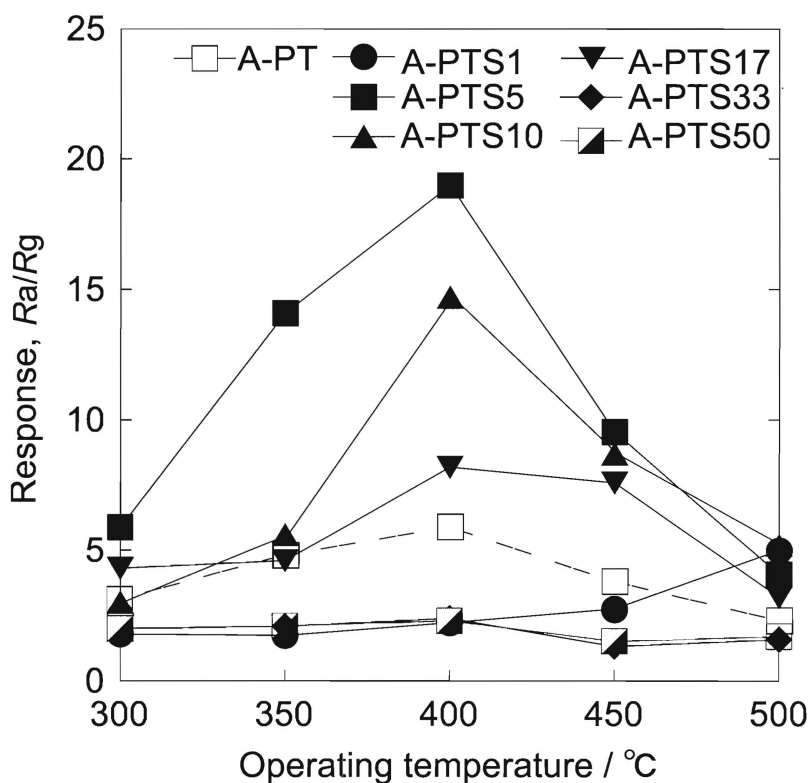

Fig. 7. Temperature dependences of response of m·mp-SnO_2 sensors with 0–50 wt% Sb_2O_5 added to 1000 ppm H_2.

4.   Conclusions

mp-SnO$_2$ and m·mp-SnO$_2$ powders with and without the addition of SiO$_2$ and/or Sb$_2$O$_5$ were prepared employing AOT and PMMA microspheres as templates and their H$_2$ sensing properties were investigated.

From the results, it was revealed that the introduction of macropores by the addition of PMMA microspheres into the mp-SnO$_2$ tends to increase the pore diameter and CS.   The addition of 5 wt% Sb$_2$O$_5$ reduced sensor resistance and the simultaneous addition of 9 wt% SiO$_2$ with Sb$_2$O$_5$ increased sensor resistance.   The large amount of macropores introduced into mp-SnO$_2$ sensors by the addition of PMMA microspheres in the preparation process markedly increased the resistance of all sensors.   The addition of Sb$_2$O$_5$ up to 10 wt% was found to reduce the sensor resistance in air, but beyond that led to an increase in sensor resistance.   Among the sensors tested, the mp-SnO$_2$ with only 5 wt% Sb$_2$O$_5$ added showed the largest response at 400°C.   The 70% response and recovery times could be reduced by the introduction of macropores.

References

1   T. Hyodo, Y. Shimizu and M. Egashira: Electrochemistry **71** (2003) 387.
2   N. Yamazoe: Sens. Actuators, B **5** (1991) 7.
3   Y. Shimizu and M. Egashira: MRS Bull. **24** (1999) 18.
4   M. Saha, A. Banerjee, A. K. Halder J. Mondal and A. Sen: Sens. Actuators, B **79** (2001) 192.
5   A. K. Mukhopadhyay and P. Mitra: Ceram. Int. **26** (2000) 123.
6   Y. Shimizu, A. Jono, T. Hyodo and M. Egashira: Sens. Actuators, B **108** (2005) 56.
7   A. Teeramong Konrasmee and M. Sriyudthsak: Sens. Actuators, B **66** (2000) 256.
8   S. Supothina: Sens. Actuators, B **93** (2003) 526.
9   S.-H. Wang, T.-C. Chou and C. Liu: Sens. Actuators, B **94** (2003) 343.
10   T. Hyodo, S. Abe, Y. Shimizu and M. Egashira: Sens. Actuators, B **93** (2003) 590.
11   T. Ishibashi, T. Hyodo, Y. Shimizu and M. Egashira: Preparation of Macroporous SnO$_2$ Thick Films and Their Application to Sensor Materials in Chemical Sensors VI, ed. C. Bruckner-Lea, P. Vanysek, G. Hunter, M. Egashira, N. Miura and F. Mizutani (Electrochemical Society, Honolulu, 2004) p. 28.
12   T. Hyodo, K. Sasahara, Y. Shimizu and M. Egashira: Sens. Actuators, B **106** (2005) 580.
13   L. Li, L. Mao and X. Duan: Mater. Res. Bull. **41** (2006) 541.
14   J. Kong, H. Deng, P. Yang and J. Chu: Mater. Chem. Phys. **114** (2009) 854.
15   D. Szczuko, J. Werner, S. Oswald, G. Behr and K. Wetzig: Appl. Surf. Sci. **179** (2001) 301.
16   H. Yang, Y. Hu and G. Qiu: Mater. Res. Bull. **37** (2002) 2453.
17   S. D. Han, H. Yang and L. Wang: Sens. Actuators, B **66** (2000) 112.
18   J. M. J. Herrman, J. T. Portefaix and M. Forissier: J. Chem. Soc. Faraday **75** (1979) 1346.